

Synthesis and Properties of a pH-Insensitive Fluorescent Nitric Oxide Cheletropic Trap (FNOCT)

by Frank Stefan Hornig^a), Hans-Gert Korth^a), Ursula Rauen^b), Herbert de Groot^b), and Reiner Sustmann^{*a})

^a) Institut für Organische Chemie der Universität Duisburg-Essen, Universitätsstr. 5, D-45117 Essen (phone: +49-201-1833097; fax: +49-201-1834259; e-mail: reiner.sustmann@uni-duisburg-essen.de)

^b) Institut für Physiologische Chemie, Universitätsklinikum Essen, D-45122 Essen

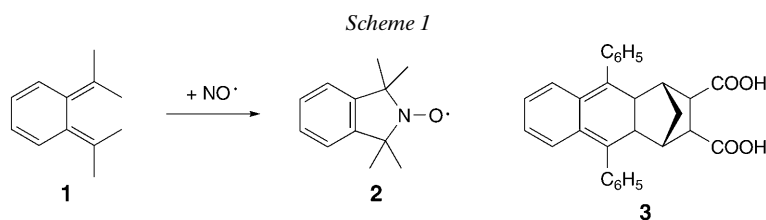
In memoriam Hanns Fischer

The synthesis and properties of the new fluorescent nitric oxide cheletropic trap (FNOCT) **14**, designed for the trapping and quantification of nitric oxide (NO) production in chemical and biological systems, is described (*Scheme 3*). The dicarboxylic acid **14** and the corresponding bis[(acetyloxy)methyl] ester derivative **15** of the FNOCT contain a 2-methoxy-substituted phenanthrene group as fluorophoric unit. The fluorescence of the reduced NO adduct of this FNOCT (λ_{exc} 320 nm, λ_{em} 380 nm) is pH-independent. Trapping experiments were carried out in aqueous buffer solution at pH 7.4 with nitric oxide being added as a bolus as well as being released from the NO donor compound MAHMA NONOate (= (1*Z*)-1-[methyl[6-(methylammonio)hexyl]amino]diazene-1,2-diolate), indicating a trapping efficiency of *ca.* 50%. In a biological application, nitric oxide was scavenged from a culture of lipopolysaccharide-stimulated rat alveolar macrophages. Under the applied conditions, a production of 11.1 ± 1.5 nmol of NO per hour and per 10^5 cells was estimated.

Introduction. – Since nitric oxide (NO) has been recognized as an important messenger molecule in mammalian cells, innumerable studies have been published on its significance in biological systems [1][2]. A highlight in this development was the Nobel prize in physiology and medicine awarded to Furchgott [3], Murad [4], and Ignarro [5] in 1997. The study of the physiological and pathophysiological functions of this simple molecule requires sensitive detection methods. A variety of methods are known to determine nitric oxide, most of them, however, are difficult to apply in living systems or are indirect assays, *i.e.*, are based on the identification of metabolites of nitric oxide [6].

We have been concerned with the development of a reaction for the direct detection of NO which we discovered in 1992 [7–10]. Although nitric oxide as a radical is rather unreactive towards organic molecules under normal conditions, it was found that it reacts readily with *o*-quinodimethanes (= 5,6-dimethylenecyclohexa-1,3-diene) to form cyclic nitroxide radicals in a kind of cheletropic reaction. This reaction is shown in *Scheme 1* for the molecule first used for this purpose, tetramethyl-*o*-quinodimethane **1** [7]. EPR Spectroscopy seemed to be the method of choice for the detection of the thus formed nitroxide **2**.

The reactive *o*-quinodimethanes were named nitric oxide cheletropic traps (NOCTs). To apply this method to biological systems, a number of problems had to



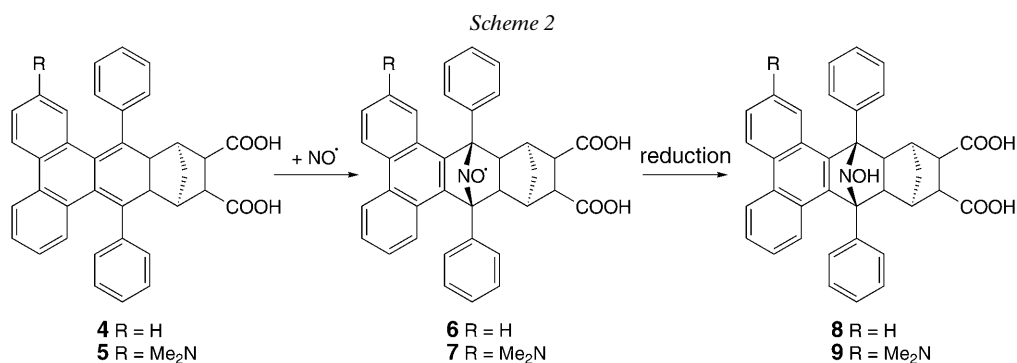
be overcome, the most important of them being the thermal stability and water solubility of the NOCT compounds. Substituted *o*-quinodimethanes had to be found which are stable enough to be applied to cellular systems in aqueous solution. According to the literature, a certain stability can be given to the *o*-quinodimethane system when typical rearrangement reactions, in particular 1,5-sigmatropic H-shifts, are suppressed. One such example has been reported [11]. In our studies, we followed this strategy and tested whether this stable, but highly reactive compound traps nitric oxide. A successful trapping experiment was achieved with NOCT derivative **3**, substituted by two carboxy groups to provide sufficient water solubility and which was sufficiently stable. The corresponding nitroxide was characterized by EPR spectroscopy [12]. The trapping kinetics, studied by stopped-flow techniques, unveiled a second-order rate constant $k_2 = 5600 \text{ M}^{-1} \text{ s}^{-1}$ at 22° in buffer solution at pH 7.4. Unfortunately, the lifetime of the produced nitroxide radical was only 100 s under these conditions, *i.e.*, too short to apply EPR detection for monitoring NO production in biological systems [13].

A further problem arose when it was realized that nitroxide radicals may be not stable in a cytosolic medium. We, therefore, turned away from EPR spectroscopy as detecting method to the more sensitive fluorescence spectroscopy. We thus developed 'fluorescent NOCTs' (FNOCTs) such as **4** (Scheme 2). By employing a phenanthrene-based *o*-quinodimethane system, a radical **6** with a fluorophoric phenanthrene moiety was formed on reaction with nitric oxide. To avoid self-quenching of fluorescence by the nitroxide radical [14], a reducing agent, *e.g.*, ascorbic acid, is added to generate the corresponding hydroxylamine derivative **8**. After reduction, the phenanthrene fluorescence can easily be detected. This FNOCT was further modified by adding a dimethylamino group in 2-position of the phenanthrene ring (\rightarrow **5**) [15]. Thereby, the excitation wavelength for the hydroxylamine product **9** (from **7**) is shifted from 315 (**8**) to 380 nm (**9**), which is advantageous for applications in cellular systems because short-wavelength excitation may damage living cells and hampers also the application due to interference with fluorescence of typical cell constituents, especially NAD(P)H.

A disadvantage of this otherwise perfect FNOCT **5** is the pH dependence of the fluorescence intensity because of the presence of the protonable dimethylamino group [15].

Here we report on the synthesis of a corresponding methoxy-substituted FNOCT which should display similar fluorescence properties as the dimethylamino-substituted compound and where the fluorescence properties should be pH-independent.

Results and Discussion. – *Synthesis of FNOCTs 14 and 15.* The 2-methoxyphenanthrene-9,10-quinone (**10**) was prepared in analogy to the literature by nitration of phenanthrene-9,10-quinone, which yielded a mixture of the 2-nitro (36%) and the 4-nitro

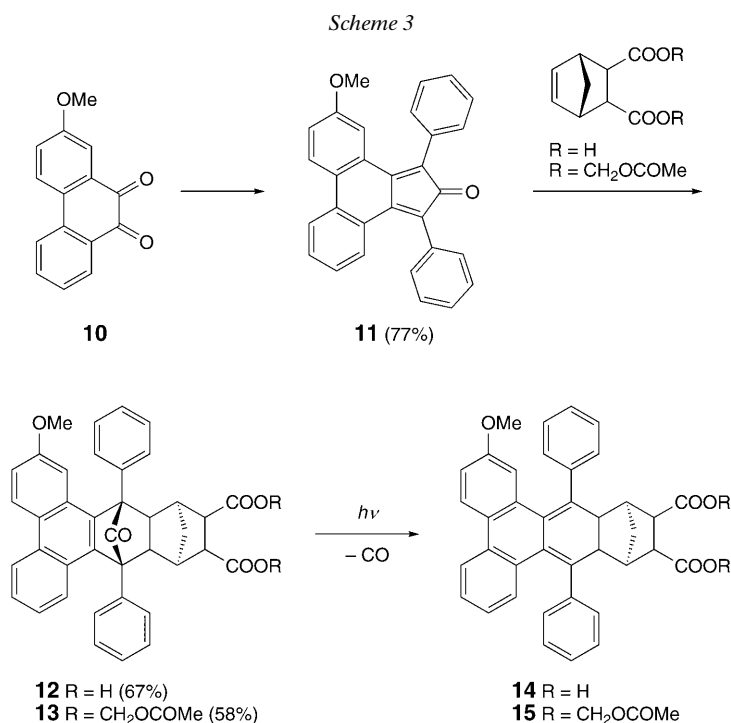


isomer (33%). The isomers could be separated due to their different solubility in EtOH and crystallization of the 2-substituted isomer from AcOH. Treatment of 2-nitrophenanthrene-9,10-quinone with sodium dithionite led to reduction of both the nitro group and the quinoid system. *In situ* air oxidation regenerated the quinone system in 71% yield. Replacement of the NH_2 by the OH group *via* diazotation and subsequent thermal decomposition of the diazonium salt gave the hydroxy compound (77%). Reaction with dimethyl sulfate gave 2-methoxyphenanthrene-9,10-quinone (**10**) in 80% yield.

Condensation of **10** with 1,3-diphenylacetone (=1,3-diphenylpropan-2-one) provided the corresponding cyclone **11** (yield 77%; Scheme 3). *Diels–Alder* reaction of **11** with norborn-5-ene-2-*endo*,3-*exo*-3-dicarboxylic acid and the corresponding (acetyloxy)methyl ester yielded the bridged ketone derivatives **12** (67%) and **13** (38%). Compounds **12** and **13** are both mixtures of two diastereoisomers in 1:1 (**12**) and 4:1 (**13**) ratio, respectively. Assignment of the isomeric structures was not attempted. The (acetyloxy)methyl ester was prepared, because this type of ester [16][17] is cell-membrane permeable and is enzymatically hydrolyzed to the corresponding carboxylates [18]. In principle, the *Diels–Alder* cycloaddition would provide a mixture of four diastereoisomers. The methoxy group renders phenyclone **11** nonsymmetrical, and both orientations of the diene and dienophile (*endo* or *exo*) may be realized. As *endo* additions to the norbornene double bond are not known, the number of possible products is reduced to racemic mixtures of two diastereoisomers of **12**. The diastereoisomer mixtures **12** and **13** were not separated as their reactivity towards nitric oxide should be similar. Recently, an X-ray analysis of a related pyrene-based cycloadduct confirmed our $^1\text{H-NMR}$ -based assignment [19].

$^1\text{H-NMR}$ Spectroscopy supports the assignment of the CO and CH_2 bridges of **12** and **13** in an '*anti*' position. Due to this configuration, the CH_2 group of the norbornane moiety is positioned below the phenanthrene skeleton. Therefore, the two CH_2 protons are differently diamagnetically shielded and appear at high field as an *AB* system for both the acid **12** and the ester **13**. The two *AB* systems of the diastereoisomers are superimposed. In case of acid **12**, one of these protons is found at $\delta -0.47$, the other at $\delta 0.52$. The low-field signal comprises two overlapping *d* with $^3J = 11.0$ and 11.2 Hz, respectively. The high-field signal appears as a slightly broadened *d*.

o-Quinodimethanes are normally unstable, reactive molecules [20]. A compound where the methylene C-atoms of the *o*-quinodimethane moiety are bound to a norbor-



nane system, forming a six-membered ring, proved to be isolable, though remained very reactive [11]. Photochemically induced removal of carbon monoxide from **12** and **13** makes such bridged *o*-quinodimethanes accessible (*Scheme 3*). It was presumed that compounds **14** and **15** would be isolable, so that they might be used as FNOCTs. To get FNOCTs which can be applied in biological situations, carbon monoxide extrusion has to be essentially quantitative, otherwise the residual ketone derivative gives rise to background fluorescence similar to that of the nitric oxide trapping product (see below). This situation required optimization of the photolysis conditions. The photolysis was carried out in a *Rayonet* photochemical reactor. Two wavelengths, 254 and 300 nm, were tested, of which only the longer-wavelength irradiation led to the desired product. In addition, formation of fluorescent by-products made it necessary to optimize the temperature of photolysis and the solvent. Therefore, only small quantities of *ca.* 20 mg were photolyzed under Ar in a quartz NMR tube which was immersed in a thermostated methanol bath (highest commercial purity). THF was found to be the solvent of choice, but it had to be absolutely dry to avoid side reactions. Deuterated THF was used to allow monitoring of the progress of the reaction by ¹H-NMR spectroscopy. The optimum photolysis temperature was –10°. In this way, conditions for temperature and reaction time were established. According to 500-MHz ¹H-NMR spectroscopy, the purity of the FNOCTs was $\geq 95\%$. Attempts to further purify products **14** and **15** after photolysis by chromatography or recrystallization were unsuccessful because of partial decomposition. Identification and characterization of **14** and **15** was carried out

by ^1H - and ^{13}C -NMR and by high-resolution mass spectrometry (ESI-TOF) (see *Exper. Part*).

For the purpose of further studies, in particular nitric oxide trapping experiments, the solvent of the photolysis solution was removed *in vacuo* and the dry, orange-red residue was stored under Ar at -20° .

UV/VIS and Fluorescence Spectroscopy. FNOCT **14** displays the typical absorption spectrum of *o*-quinodimethanes. *Fig. 1* shows the long-wavelength absorption band with a maximum at λ_{max} 445 nm and $\log \epsilon = 3.63$. This absorption disappears readily on reaction with nitric oxide indicating conversion of the quinoid π -system to the aromatic phenanthrene system. The disappearance of this band was monitored in stopped-flow kinetic measurements of the reaction of FNOCT with nitric oxide (see below).

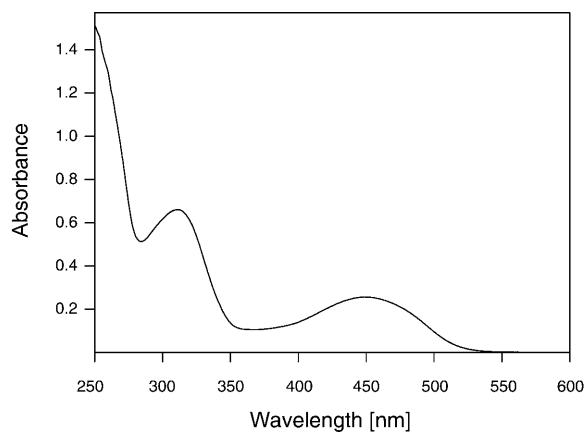


Fig. 1. UV/VIS Spectrum of *o*-quinodimethane derivative **14** in THF. [**14**] = 50 μM , T 20 $^\circ$.

In previous studies on phenanthrene-based FNOCTs, it was observed that the FNOCT with an unsubstituted phenanthrene ring did not fluoresce [21], whereas FNOCT **5** carrying a dimethylamino group in 2-position of the fluorophoric unit displayed a fluorescence at a longer wavelength, *viz.* λ_{em} 600 nm (λ_{exc} 450 nm) [15], than the NO-trapping product. The intensity of this fluorescence is an order of magnitude lower than that of the parent ketone or the reduced NO-trapping product. Similarly, a weak fluorescence was also found for the methoxy-substituted FNOCTs **14** and **15** in THF solution, as shown in *Fig. 2* for **14**. The spectra of both the acid and the (acetyloxy)methyl ester were essentially identical.

NO Trapping and EPR Spectroscopy. The reaction of FNOCTs **14** and **15** with NO to give nitroxides **16** and **17**, respectively (*Scheme 4*) was studied by EPR spectroscopy. For this purpose, a 4 mM solution of the FNOCT in THF, freshly prepared by photolysis of the corresponding bridged ketone derivative, was treated with an excess of NO by adding an NO-saturated THF solution. The solutions were made oxygen-free to avoid autoxidation of nitric oxide.

The EPR spectra of **16** and **17** were identical. *Fig. 3* shows the spectrum of nitroxide **16** as produced from acid **14**. The EPR spectrum is characterized by a large N hyperfine splitting constant of $a(^{14}\text{N}) = 2.284$ mT and a g value of 2.00634, both very characteristic

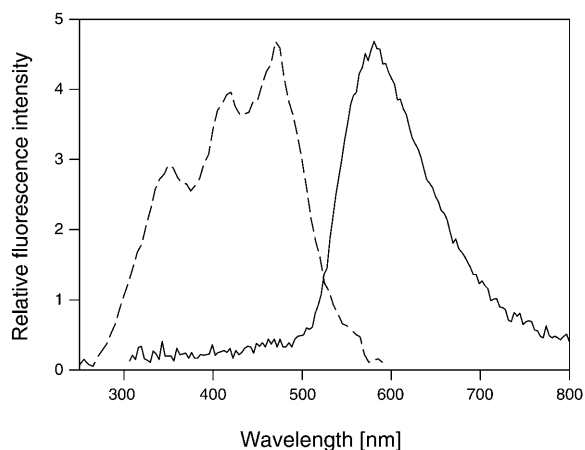
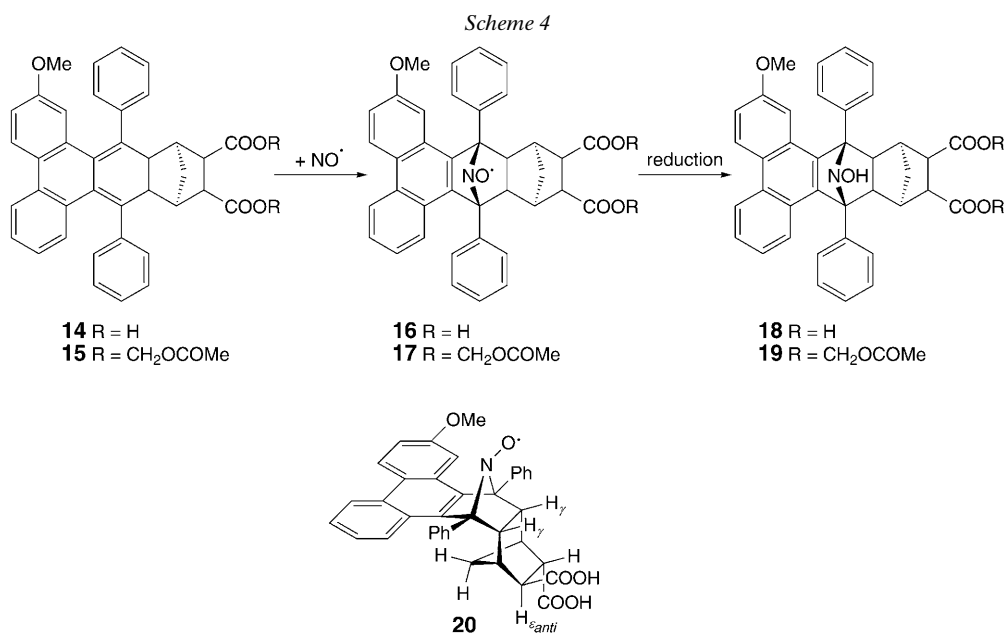


Fig. 2. Excitation and emission spectrum of **14** in THF. [**14**] = 50 μ M, λ_{exc} 470 nm, λ_{em} 580 nm.



for bridged nitroxides [22]. The N hyperfine lines show an additional q splitting of $a(\text{H})=0.074$ mT for three equivalent H-atoms. These splittings are attributed to an interaction of the unpaired spin with norbornane H-atoms, the two bridgehead γ -protons and one proton in ϵ -position. The accidentally identical splitting constants indicate a double W -arrangement of the ϵ -proton relative to the unpaired electron at the nitroxide group. This supports structure **20** (*Scheme 4*) for the nitroxide radical **16** with the nitroxide group and the CH₂ bridge in 'anti' position and establishes the attack of NO at the less hindered side of the FNOCT plane.

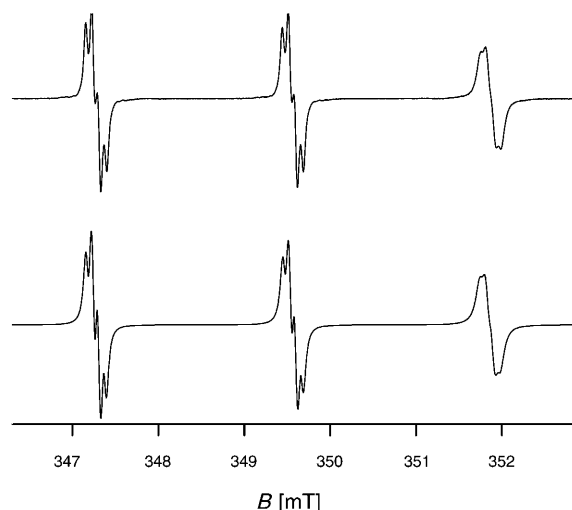


Fig. 3. Experimental (top) and simulated (bottom) EPR spectrum of nitroxide radical **16** in THF. $g = 2.00634$, $a(^{14}\text{N}) = 2.284$, $a(\text{H}_\gamma) = 0.074$, $a(\text{H}_\epsilon) = 0.074$ mT; $T 23^\circ$.

Fluorescence Spectroscopy of the Reduced NO-Trapping Products 18 and 19. To overcome the self-quenching of the fluorescence of the nitroxide, NO addition (saturated THF solution) was carried out in the presence of a slight molar excess of ascorbic acid as reducing agent. By this means radicals **16** and **17** were rapidly reduced to the corresponding hydroxylamine derivatives **18** and **19**, respectively. As expected, the fluorescence spectrum of hydroxylamine derivative **18**, recorded in phosphate buffer solution at pH 7.2 (Fig. 4), is very similar to that of the parent bridged ketone derivative **12** (spectrum not shown) prior to photolysis to FNOCT **14**.

Two excitation wavelengths were probed, λ_{exc} 320 and 350 nm, giving rise to the same emission spectrum (Fig. 4, upper and lower trace, resp.). Compared to the 2-(dimethylamino)-substituted FNOCT **5** and its NO trapping product **9**, the excitation and emission maxima are located at shorter wavelengths. This suggests that biological applications might be hampered by the autofluorescence of cell constituents, in particular by that of NAD(P)H.

Stopped-Flow Measurements. The rate of reaction of FNOCT **14** with nitric oxide was determined by stopped-flow UV measurements in THF, following the decay of the maximum of the *o*-quinoid absorption at 445 nm. The measurements were carried out at 21° under pseudo-first-order conditions by using a 10-to-100-fold excess of nitric oxide. A second-order rate constant $k_2 = 750 \pm 11 \text{ l mol}^{-1}\text{s}^{-1}$ was obtained. This magnitude is comparable to that found for the 2-(dimethylamino)-substituted phenanthrene FNOCT [15]. Similar to the previous FNOCTs it is expected that the rate constant in aqueous buffer will be somewhat lower due to solvation effects. Although the rate is several powers of ten lower than the value for reaction of NO with biological molecules like heme systems, it will be sufficient for the detection of NO in living systems, as has been demonstrated before [23]. Moreover, a partial trapping of NO may even be advantageous as only a small perturbation of the cellular function of NO will be exerted.

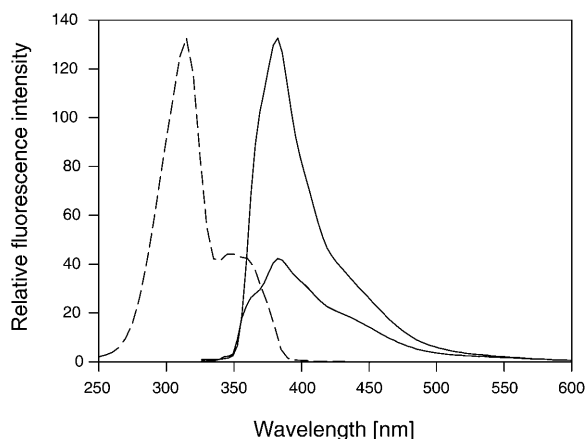


Fig. 4. Excitation (dashed line) and emission spectrum (solid lines) of hydroxylamine derivative **18** from reaction of **14** with NO in the presence of ascorbic acid in phosphate buffer pH 7.20. [phosphate buffer] = 50 mM, [ascorbic acid] = 100 μ M, [**14**] = 50 μ M. Upper and lower trace of emission spectrum from excitation at λ_{exc} 320 and 350 nm, respectively; λ_{em} 385 nm.

Properties and Applications of FNOCTs 14 and 15. FNOCTs **14** and **15** were conceived to eliminate the pH dependence of the fluorescence intensity of the (dimethylamino)-substituted FNOCT **5** [15]. The pH insensitivity of the fluorescence was established in oxygen-free buffer solution at pH 5.6 (acetate buffer), 7.35 (phosphate buffer), and 9.0 (borate/KCl/NaOH buffer) with the FNOCT-precursor ketone **12** since its fluorescence characteristics is identical to that of the NO-trapping product **18**. Under standard settings of the fluorimeter (see *Exper. Part*), the fluorescence intensities from 50 μ M solutions was identical at all the three pH values (data not shown).

To check the trapping efficiency for NO, 50 μ M solutions of FNOCT **14** in oxygen-free phosphate buffer pH 7.35 were mixed with increasing aliquots of a saturated (*ca.* 2 mM) aqueous NO solution. The upper trace in *Fig. 5* displays the dependence of the fluorescence intensity on the concentration of NO in the absence of oxygen, measured 15 min after addition of the NO stock solution. Saturation of the fluorescence intensity, corresponding to a complete consumption of FNOCT **14**, is reached at an approximately three-fold excess of NO. Hence, under the employed conditions, side reactions seem to take place which lead to a reduced trapping efficiency for NO. If FNOCT and NO are present in equimolar amounts *ca.* 50% of the added NO is trapped. This amount decreases even further if the trapping experiment is carried out in air-saturated buffer (*Fig. 5*, lower trace). A reduced trapping efficiency in the presence of oxygen has been found for other FNOCTs as well and reflects the competing autoxidation of NO.

In addition to the study of NO trapping with NO being added as a bolus, we assessed the trapping of continuously generated NO by utilizing the NO donor MAHMA NONOate (= (1*Z*)-1-[methyl[6-(methylammonio)hexyl]amino]diazene-1-ium-1,2-diolate = 6-(2-hydroxy-1-methyl-2-nitrosohydrazino)-*N*-methylhexan-1-amine). With regard to the envisaged studies in biological systems, these measurements were performed at 37° in air-saturated phosphate buffer (50 mM, pH 7.4) in the presence of 100 μ M of the iron chelator diethylenetriaminepentaacetic acid (= *N,N*-bis[2-[bis(car-

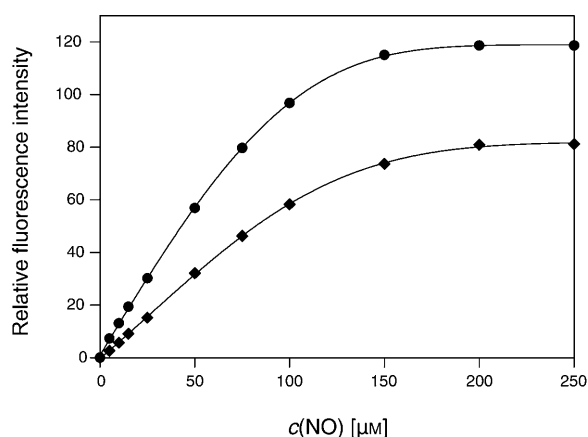


Fig. 5. NO Trapping by FNOCT **14** as a function of added NO at pH 7.35. [**14**] = 50 µM, [phosphate buffer] = 50 mM, [ascorbic acid] = 100 µM; ● oxygen-free buffer, ◆ air-saturated buffer.

boxymethyl)amino]ethyl]glycine; dtpa) and the reductant 6-hydroxy-2,5,7,8-tetramethylchroman-2-carboxylic acid (=3,4-dihydro-6-hydroxy-2,5,7,8-tetramethyl-2H-1-benzopyran-2-carboxylic acid = *Trolox*), a water-soluble analogue of vitamin E, and with a lower concentration of FNOCT **14**, *i.e.*, 10 µM (see below). The time evolution of the fluorescence of the reduced NO adduct **18** was followed for a range (0–100 µM) of MAHMA NONOate concentrations (*Fig. 6*). For all concentrations of MAHMA NONOate, the time dependence of fluorescence obeys a clean first-order rate law, reflecting the rate of decomposition of MAHMA NONOate. From the least-squares fits displayed in *Fig. 6*, an average rate constant for NO release from MAHMA NONOate of $k^{310K} = (7.8 \pm 0.8) \cdot 10^{-3} \text{ s}^{-1}$ as evaluated, corresponding to a half-life of 1.5 min under these conditions. This value agrees well with the half-life of MAHMA NONOate of 2.7 min at 22° as given in the literature [24]. Hence, FNOCTs **14** and **15** can advantageously be used for kinetic studies of NO-releasing compounds.

As in the experiments with NO solution, fluorescence intensity (as determined after complete decomposition of the NO donor after > 15 min) increased with increasing MAHMA NONOate concentrations (*Fig. 7*). Again, saturation was observed, albeit a larger excess of NO was required to reach saturation: even with 40 µM MAHMA NONOate, *i.e.*, an eightfold excess of NO, saturation was not yet complete.

As to be expected, the trapping efficiency increased with increasing concentrations of FNOCT **14** (*Fig. 8*). Maximal trapping of NO generated by 0.5–5 µM MAHMA NONOate (= 1–10 µM NO) was observed with 50 µM FNOCT **14**, at higher concentrations of the trap, *i.e.*, 100 µM, the fluorescence intensity was slightly decreased, probably due to photophysical quenching effects.

With 10 µM FNOCT **14**, *i.e.*, with the concentration of **14** later applied in a cellular system (see below), the NO release by 0.2–2 µM MAHMA NONOate (= 0.4–4 µM NO) could be readily measured with a microplate reader as often used for biological applications (sample volume 300 µl); monitoring of lower NO levels proved to be too strongly obscured by background fluorescence to allow reliable measurements.

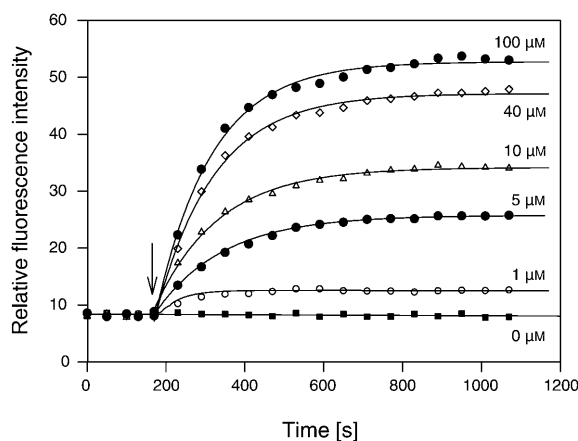


Fig. 6. Time evolution of NO release from MAHMA NONOate as monitored by trapping with FNOCT **14** at pH 7.4. [**14**]=10 μM , [phosphate buffer]=50 mM, [Trolox]=100 μM , [dtpa]=100 μM ; λ_{exc} 320 nm, λ_{em} 380 nm; T 37°. The arrow marks the point of addition of MAHMA NONOate; numbers indicate the initial concentration of MAHMA NONOate. Solid lines are least-squares fits to a first-order rate law.

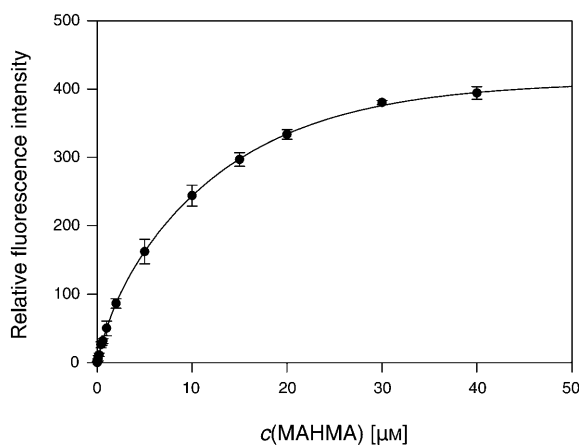


Fig. 7. Efficiency of NO trapping by FNOCT **14** at pH 7.4 as a function of the concentration of the NO donor MAHMA NONOate. [**14**]=10 μM , [phosphate buffer]=50 mM, [Trolox]=100 μM , [dtpa]=100 μM ; λ_{exc} 320 nm, λ_{em} 380 nm; T 37°.

For 0.2–0.6 μM MAHMA NONOate, trapping efficiency was above 50% (up to 65%) and with 1–2 μM MAHMA NONOate between 40 and 50%.

Trapping of NO Produced from Isolated Macrophages. As an example of NO-producing cells, cultured rat alveolar macrophages, *i.e.*, nonspecific immune cells isolated from the rat lung, were used. These cells can be activated *in vitro* by bacterial lipopolysaccharides (LPS) to express the enzyme inducible nitric oxide synthase (iNOS) and then to produce considerable amounts of NO. Unfortunately, FNOCT **14** displayed cytotoxicity when applied to the alveolar macrophages in the optimal trapping concen-

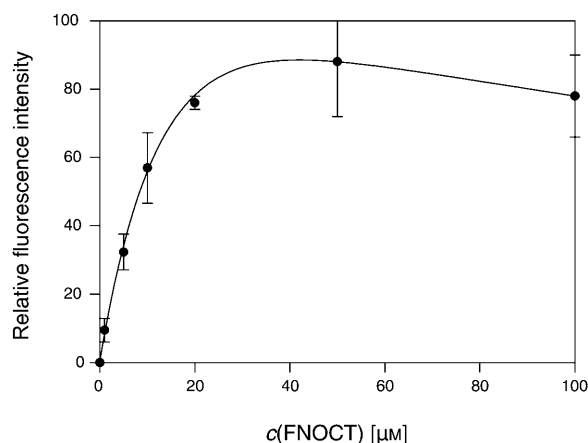


Fig. 8. Efficiency of NO trapping at pH 7.4 as a function of the concentration of FNOCT **14**. [MAHMA NONOate] = 1 μM , [phosphate buffer] = 50 mM, [Trolox] = 100 μM , [dtpa] = 100 μM ; λ_{exc} 320 nm, λ_{em} 380 nm; T 37°.

tration of 50 μM (see above). Therefore, a concentration of 10 μM FNOCT **14** was used in all cellular applications. At this concentration, no significant cell death was observed within the duration of the experiments. As a reductant to be used in the cellular system, the H₂O-soluble vitamin-E analogue *Trolox* proved to be advantageous because reduction of nitroxide radical **16** to the fluorescent hydroxylamine **18** was found to be much more rapid with *Trolox* (100 μM) than with glucose (10 mM), the reductant used in previous biological studies [23]. Ascorbate, the preferred reductant in most of the chemical experiments (see above), was found to increase the background fluorescence over time, thus turned out to be unfavorable for cellular systems where NO is produced rather slowly and at low levels, requiring prolonged incubation periods for NO trapping. The (extracellular) iron chelator diethylenetriaminepentaacetic acid (dtpa, 100 μM) was found to suppress the slow increase of the background fluorescence observed during prolonged incubation periods and was, therefore, added to all buffers used for cellular measurements. Under these conditions, a strong increase in fluorescence intensity could be observed in the supernatant of LPS-activated alveolar macrophages following 1 h of incubation with FNOCT **14**. This increase in fluorescence intensity was undoubtedly due to trapping of NO, as it was not observed in the supernatant of LPS-activated cells incubated with FNOCT **14** in the presence of the NOS inhibitor *N*^G-monomethyl-L-arginine (= *N*²-[imino(methylamino)methyl]-L-ornithine; NMA). Similarly, nonactivated cells did not increase fluorescence intensity to a considerable extent. Additional experiments were performed in which a large excess of MAHMA NONOate (100 μM) was added to the supernatant samples after cellular NO production had been measured. Comparison of the thus obtained fluorescence intensities with those from similar experiments performed with cell lysates (cells were lysed with sodium dodecyl sulfate (SDS), final concentration 0.4%, at the end of the experiments) revealed that after 1 h of incubation, $32 \pm 4\%$ of the applied FNOCT **14** was strongly associated with the cells, *i.e.*, incorporated in the cells and/or bound to cellular membranes. The data shown in Fig. 9 are total fluorescence, *i.e.*, fluorescence from the supernatant plus fluorescence

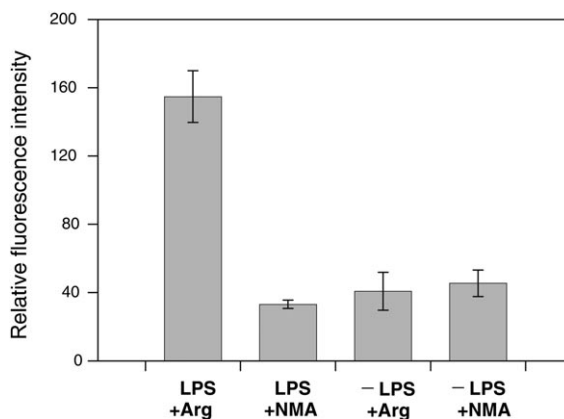


Fig. 9. Trapping of NO produced by rat alveolar macrophages. **LPS + Arg**: Cells activated with LPS (0.5 $\mu\text{g/ml}$, 18 h) in the presence of L-arginine (0.5 mM); **LPS + NMA**: Cells activated with LPS (0.5 $\mu\text{g/ml}$, 18 hrs) in the presence of the NO-synthase inhibitor NMA (0.1 mM); **-LPS + Arg**: Cells incubated with L-arginine (0.5 mM), no pretreatment with LPS; **-LPS + NMA**: Cells incubated with NMA (0.1 mM), no pretreatment with LPS. All experiments were performed in *Krebs-Henseleit* buffer, $[\text{D-glucose}] = 10 \text{ mM}$, $[\text{dtpa}] = 100 \mu\text{M}$, $[\text{Trolox}] = 100 \mu\text{M}$, $[\mathbf{14}] = 10 \mu\text{M}$; incubation time 1 h, $T 37^\circ$. Fluorescence intensity ($\lambda_{\text{exc}} 320$, $\lambda_{\text{em}} 380 \text{ nm}$) shown is the sum of the fluorescence from the supernatant and cell-associated fluorescence as determined in the cell lysates (corrected for volume, background, and cell density).

from the lysate, corrected for background fluorescence, volume, and cell density. The increase in fluorescence due to NO production from activated cells (in the absence of the NOS inhibitor) was observed in the supernatant as well as in the cell lysate.

Estimation of the amount of NO produced by the cells by using the calibration curve shown in *Fig. 7* yielded a NO production of $11.1 \pm 1.5 \text{ nmol h}^{-1} (10^5 \text{ cells})^{-1}$ in LPS-activated, noninhibited cells, $1.3 \pm 0.1 \text{ nmol h}^{-1} (10^5 \text{ cells})^{-1}$ in LPS-activated, NOS-inhibited cells, $1.6 \pm 0.5 \text{ nmol h}^{-1} (10^5 \text{ cells})^{-1}$ in nonactivated cells, and $1.8 \pm 0.3 \text{ nmol h}^{-1} (10^5 \text{ cells})^{-1}$ in nonactivated, NOS-inhibited cells. The NO produced in the activated, non-inhibited cells was trapped to *ca.* 30% in the cells and to *ca.* 70% in the cellular supernatant, a finding that fits well with the distribution of the NO trap (see above).

The foregoing experiments demonstrate that FNOCT **14** can be successfully used in cellular/biological systems to trap endogenously produced NO and to estimate cellular NO production, although there are still some limitations with regard to sensitivity and toxicity (use of higher concentrations of the trap would be desirable to achieve higher trapping efficiencies).

Biological applications of the (acetyloxy)methyl ester FNOCT **15** are currently in progress.

The excellent technical assistance of Ms *N. Boschenkov* is gratefully acknowledged.

Experimental Part

General. The following compounds were prepared according to published procedures: 2-nitrophenanthrene-9,10-quinone [25], 2-aminophenanthrene-9,10-quinone [26], 2-hydroxyphenanthrene-9,10-quinone [27], 2-methoxyphenanthrene-9,10-quinone (**10**) [28], chloromethyl acetate [29], dimethyl norborn-5-ene-2-endo,3-exo-dicarboxylate (=dimethyl bicyclo[2.2.1]hept-5-ene-2-endo,3-exo-dicarboxylate) [30], norborn-5-ene-2-endo,3-exo-dicarboxylic acid (=bicyclo[2.2.1]hept-5-ene-2-endo,3-exo-dicarboxylic acid) [31]. M.p.: uncorrected. UV/VIS: *Varian Cary 300 Bio*; λ_{\max} [nm] (log ϵ). Fluorescence: *J&M FL3095*. Fluorescence microplate reader: *BMG Labtech FLUOstar Optima*. Stopped flow: *HITech-Scientific Ltd SF41*. IR: *Bio-Rad Series FTS 135 FT-IR*; in cm^{-1} . ^1H - and ^{13}C -NMR Spectra: *Bruker DRX 500* and *Varian Gemini 200*; δ in ppm, I in Hz; an asterisk (*) denotes signals of a second isomer. EPR: *Bruker ESP 300E*. MS: *Bruker BioToF II*. Elemental analyses: *Elektrothermal 9100*.

5-Methoxy-1,3-diphenyl-2H-cyclopenta[1]phenanthrene-2-one (11). A mixture of **10** (1.50 g, 6.30 mmol) and 1,3-diphenylpropan-2-one (1.30 g, 6.18 mmol) in EtOH (100 ml) was heated to 35°. To this suspension was added within 30 min 3.5M KOH in EtOH (20 ml). Five minutes after complete addition, the black precipitate was filtered and washed once with a small amount of EtOH: 2.00 g (77% of **11**). M.p. 237°. UV (THF): 632 (3.19), 499 (2.99), 442 (3.30), 305 (4.75), 264 (4.68). IR (KBr): 3070, 3002, 2900, 2830, 1693, 1599. ^1H -NMR (500 MHz, CDCl_3): 7.74 (*d*, $^3J=7.57$, 1 H); 7.67 (*d*, $^3J=8.51$, 1 H); 7.45 (*d*, $^3J=7.73$, 1 H); 7.46–7.27 (*m*, 10 H); 7.21 (*t*, $^3J=7.88$, 1 H); 7.00 (*d*, $^4J=2.37$, 1 H); 6.85 (*t*, $^3J=7.72$, 1 H); 6.80 (*dd*, $^3J=8.52$, $^4J=2.22$, 1 H); 3.33 (*s*, MeO). ^{13}C -NMR (125 MHz, CDCl_3): 200.3; 159.1; 148.5; 148.3; 137.7; 133.8; 131.4; 125.8; 119.3; 119.0; 107.6; 111.9; 128.5; 128.1; 127.7; 127.3; 126.4; 126.7; 127.2; 54.7 (MeO). HR-ESI-MS: 413.1567 (M^+ , $\text{C}_{30}\text{H}_{21}\text{O}_2^+$; calc. 413.1536).

Bicyclo[2.2.1]hept-5-ene-2-endo,3-exo-dicarboxylic Acid Bis[(acetyloxy)methyl] Ester. To norborn-5-ene-2,3-dicarboxylic acid (4.55 g, 25.0 mmol) in dimethylformamide (50 ml), dried by filtration through neutral Al_2O_3 , was added in 10 portions NaH suspension in paraffine (2.40 g, 100 mmol). Within 30 min, chloromethyl acetate (5.42 g, 50.0 mmol), kept at -10° , was added dropwise into this soln. After 3 h at 40° , the mixture was freed of surplus NaH by filtration. After evaporation of the solvent at r.t./10 Pa, the residue was bulb-to-bulb distilled at $130^\circ/10$ Pa: 3.83 g (47%). ^1H -NMR (200 MHz, CDCl_3): 6.31 (*m*, 1 H); 6.05 (*m*, 1 H); 5.85–5.30 (*m*, 2 OCH_2O); 3.45 (*t*, $^3J=4.2$, 1 H), 3.32 (*br. s*, 1 H); 3.15 (*br. s*, 1 H); 2.74 (*dd*, $^3J=4.3$, 1 H); 2.14–2.05 (*d*, 2 Me); 1.70–1.49 (*m*, 2 H).

9,9a,10,11,12,13,13a,14-Octahydro-2-methoxy-15-oxo-9,14-diphenyl-9,14:10,13-dimethanobenzol[b]triphenylene-11,12-dicarboxylic Acid (12). A suspension of **11** (1.00 g, 2.42 mmol) and bicyclo[2.2.1]hept-5-ene-2-endo,3-exo-dicarboxylic acid (0.459 g, 2.52 mmol; *ca.* 4% excess) in chlorobenzene (25 ml) was refluxed for 8 h in the dark under Ar. After filtration at r.t., the residue was dissolved in THF (*ca.* 130 ml) at slightly elevated temp. To the soln., charcoal (0.3 g) was added. After stirring for 30 min, the charcoal was filtered off, the solvent evaporated, and the product precipitated by addition of a 10-fold excess of heptane: 0.95 g (67%) of **12** as a 1:1 diastereoisomer mixture. M.p. 293°. UV (THF): 350 (2.78), 343 (3.00), 313 (3.94), 267 (4.77). IR (KBr): 3318, 3063, 3028, 2835, 2968, 2911, 1768, 1736, 1703, 1615, 1173, 1093. ^1H -NMR (500 MHz, $(\text{D}_8)\text{THF}$): 11.29 (*br. s*, 2 H, COOH); 8.67 (*t*, $^3J=9.0$, 1 H); 8.19–7.89 (*dd*, $^3J=7.89$, 1 H); 7.71–7.57 (*m*, 2 H); 7.48–7.06 (*m*, 11 H); 6.63 (*d*, $^4J=3.0$, 1 H); 3.27, 3.26* (*s*, 3 H, MeO); 3.26–3.23 (*m*, 2 H); 3.06 (*m*, 1 H); 3.23–3.13 (*m*, 2 H); 2.95–2.83 (*m*, 1 H); 0.52 (*dd*, $^2J=11.8$, 1 H); -0.47 (*dd*, $^3J=11.5$, 1 H). ^{13}C -NMR (125 MHz, $(\text{D}_8)\text{THF}$): 199.0; 174.8; 174.1; 158.9; 138.8; 138.5; 138.4*; 138.1; 136.3; 136.1*; 135.0; 134.8*; 132.8; 132.6*; 129.6*; 127.2; 126.2; 130.1; 130.0; 129.9*; 129.8; 129.4; 129.3*; 129.1; 129.0*; 128.9; 128.8*; 128.7; 127.8; 127.7*; 126.1; 126.0*; 125.9; 125.8*; 125.7; 123.8; 118.6; 118.5*; 106.1; 106.0*; 64.6; 64.4; 64.1; 64.0; 54.8 (MeO); 51.9; 51.8; 51.2; 48.4; 48.2*; 45.5; 44.4; 44.3; 43.1; 34.7 ($\text{C}(10^\circ)$). HR-ESI-MS: 617.1945 ($[M+\text{Na}]^+$, $\text{C}_{39}\text{H}_{30}\text{NaO}_6^+$; calc. 617.1935).

9,9a,10,11,12,13,13a,14-Octahydro-2-methoxy-15-oxo-9,14-diphenyl-9,14:10,13-dimethanobenzol[b]triphenylene-11,12-dicarboxylic Acid Bis[(acetyloxy)methyl] Ester (13). Under Ar and in the dark, **11** (200 mg, 0.48 mmol) and bicyclo[2.2.1]hept-5-ene-2-endo,3-exo-dicarboxylic acid bis[(acetyloxy)methyl] ester (158.2 mg, 0.48 mmol) were heated under reflux in chlorobenzene (5 ml) for 4 h. A residual black solid was filtered off and discarded. Chlorobenzene was evaporated. The remaining brownish oil was dissolved in THF (10 ml) and the product was precipitated from the soln. by the slow addition of

heptane (100 ml). The yellow suspension was stirred for 5 h, after which the product was isolated by filtration: 0.203 g (58%) of **13**, 4:1 diastereoisomer mixture (*: minor component). M.p. 209°. UV (THF): 361 (3.13), 344 (3.18), 313 (3.93), 266 (4.69). IR (KBr): 3056, 3028, 2835, 2968, 2927, 1768, 1732, 1614, 1170. ¹H-NMR (500 MHz, (D₈)THF): 8.68 (*d*, ³*J*=8.1, 1 H); 8.66 (*d*, ³*J*=7.7, 1 H); 8.05–7.87 (*m*, 2 H); 7.75–7.64 (*m*, 2 H); 7.49–7.07 (*m*, 10 H); 6.61, 6.57* (*d*, ³*J*=3.0, 1 H); 5.96–5.90* (*m*, 1 H, OCH₂O); 5.68–5.61 (*m*, 2 H, OCH₂O); 3.31–3.25 (*m*, 3 H); 3.28, 3.26* (*s*, 3 H, MeO); 3.25, 3.23* (*d*, ³*J*=4.1, 1 H); 3.05, 2.98* (*d*, ³*J*=3.8, 1 H); 2.86, 2.82* (*s*, 1 H); 2.01, 1.98*, 1.97*, 1.95 (*s*, 6 H, Me); 0.52 (*d*, ²*J*=11.7, 1 H); –0.43 (*d*, ²*J*=10.1, 1 H). ¹³C-NMR (125 MHz, (D₈)THF): 198.7; 172.4; 171.6; 169.8; 169.5; 159.03; 158.99*; 138.5; 138.2*; 138.1*; 137.8; 136.2*; 135.9; 135.0; 134.7*; 132.8*; 132.7; 130.2; 130.06*; 130.05; 130.1*; 130.0; 129.5*; 129.4; 129.2; 129.1*; 129.0; 128.8; 128.7; 128.6; 128.42; 128.37; 128.32; 128.27; 127.8*; 127.6; 127.3; 126.2*; 126.0; 125.9*; 125.8; 123.9; 118.6; 106.0; 80.59; 80.62; 80.68; 80.75 (OCH₂O); 64.0; 64.2; 64.3; 64.5; 54.9 (MeO); 51.7*; 51.1; 48.1*; 47.9; 45.2; 44.4; 44.3*; 43.2; 20.5; 20.3* (Me). HR-ESI-MS: 761.2356 ([*M*+Na]⁺, C₄₅H₃₈NaO₁₀⁺; calc. 761.2358).

9,9a,10,11,12,13,13a-Octahydro-2-methoxy-9,14-diphenyl-10,13-methanobenzo[b]triphenylene-11,12-dicarboxylic Acid (14). Acid **12** (22.7 mg, 3.18·10⁻² mmol) was dissolved in (D₈)THF (1.0 ml) in a quartz NMR tube. Photolysis was carried out in a Rayonet photochemical reactor at 300 nm and at –10°. After 24 h, the conversion of **12** was 100% (checked by 500-MHz ¹H-NMR). The orange soln. was transferred to a Schlenk vessel and the solvent evaporated at 10 Pa. The orange **14**, a 1:1 diastereoisomer mixture, was stored in a freezer (–20°) or at –78° (dry ice). M.p. 160–165. UV (THF): 214 (4.51), 245 (4.50), 311 (4.12), 449 (3.71). IR (KBr): 3317 (OH), 2821 (MeO), 1731, 1704, 1599, 1179, 942. ¹H-NMR (500 MHz, (D₈)THF): 7.65 (*d*, ³*J*=8.5, 1 H); 7.48 (*d*, ³*J*=8.5, 1 H); 7.44–7.37 (*d*, ³*J*=8.7, 1 H); 7.41 (*d*, ³*J*=7.1, 1 H); 7.36 (*d*, ³*J*=7.2, 1 H); 7.24–7.03 (*m*, 8 H); 6.71–6.64 (*m*, 3 H); 3.21, 3.18* (*s*, 3 H, MeO); 3.31–3.22 (*m*, 3 H); 2.97–2.94 (*m*, 1 H); 2.86–2.84 (*m*, 1 H); 2.74 (*d*, *J*=3.6, 1 H); 2.14 (*m*, 1 H); 1.60 (*dd*, ³*J*=10.5, 1 H). ¹³C-NMR (125 MHz, (D₈)THF): 175.4; 175.3; 159.1; 159.2*; 144.4; 144.2*; 143.3*; 143.2; 135.7*; 135.5; 135.4; 135.3; 135.2; 135.1*; 133.90; 133.86*; 133.2; 132.8; 132.5; 130.8*; 130.7; 130.6*; 130.5; 129.7*; 129.6; 129.2; 129.0*; 128.4; 128.3; 128.1; 126.3; 126.2*; 125.4; 123.6; 116.5; 115.7; 68.2; 67.9; 53.0 (MeO); 54.9*; 54.7; 52.4*; 52.3; 50.7*; 50.5; 48.6; 48.2*; 47.5; 34.9*; 34.75. HR-ESI-MS: 566.2046 (*M*⁺, C₃₈H₃₀O₅⁺; calc. 566.2010).

9,9a,10,11,12,13,13a,14-Octahydro-2-methoxy-9,14-diphenyl-10,13-methanobenzo[b]triphenylene-11,12-dicarboxylic Acid Bis[(acetyloxy)methyl] Ester (15). As described for **14**, with **13** (20.2 mg, 2.78·10⁻² mmol) in (D₈)THF (1.0 ml) for 18 h. The orange **15**, a 4:1 diastereoisomer mixture (*: minor component) was stored in a freezer (–20°) or at –78° (dry ice). M.p. 75–77°. UV (THF): 246 (4.63), 309 (4.24), 446 (3.78). IR (KBr): 3055, 3024, 2835, 2968, 2927, 1745, 1613, 1163. ¹H-NMR (500 MHz, (D₈)THF): 7.66–7.63 (*m*, 2 H); 7.48–7.44 (*d*, ³*J*=8.5, 1 H); 7.44–7.39 (*d*, ³*J*=8.4, 1 H); 7.36–7.29 (*m*, 3 H); 7.26–7.16 (*m*, 4 H); 7.09–7.02 (*m*, 2 H); 6.73–6.65 (*s*, 2 H); 6.64, 6.63* (*s*, 1 H); 5.82–5.58 (*m*, 4 H, OCH₂O); 3.36–3.32 (*m*, 1 H); 3.32–3.25 (*m*, 3 H); 3.18, 3.23* (*s*, 3 H, MeO); 3.01–3.03 (*m*, 1 H); 2.79 (*d*, ³*J*=4.1, 1 H); 2.17 (*d*, ²*J*=10.6, 1 H); 2.03, 2.01*, 1.99, 1.97* (*s*, 6 H, Me); 1.60 (*d*, ²*J*=10.9, 1 H). ¹³C-NMR (125 MHz, (D₈)THF): 172.7; 172.0; 169.5; 169.4; 159.2*; 159.1; 144.2; 144.1*; 143.1; 135.2; 134.9; 134.5; 133.6; 133.2; 132.8; 132.6*; 130.74; 130.67; 130.57*; 130.3; 129.8; 129.7*; 129.4; 128.5; 128.3*; 126.4; 126.3*; 125.4; 123.7; 116.6; 115.8; 115.7; 80.5; 80.4* (OCH₂O); 68.0; 67.9 (C(3°), C(6°)); 54.9; 54.8 (MeO); 52.1; 52.0; 50.4*; 50.3; 49.8*; 49.7; 48.5; 48.0; 34.7; 20.4; 20.3* (Me). HR-ESI-MS: 733.2420 ([*M*+Na]⁺, C₄₄H₃₈NaO₉⁺; calc. 733.2408).

Fluorescence Measurements. Fluorescence spectra were recorded at r.t. in 1-cm cuvettes. Stock solns. of the compounds (5 mM) in oxygen-free DMSO were added to the buffer to give a 50 μM final concentration.

ESR Measurements. X-Band ESR spectra were recorded in Ar-flushed, septum-capped 4-mm o.d. quartz tubes by injecting 30 μl of a sat. NO soln. in THF (30 μl) to 1 mM FNOCT in oxygen-free THF. Microwave frequency 9.48 GHz, microwave power 2 mW, modulation amplitude 0.03 mT, sweep range 7 mT, sweep time 15 min. Spectra simulation was performed by the WinSim program [32].

NO Trapping from MAHMA NONOate. These experiments were performed in nondeoxygenated sodium phosphate buffer (50 mM, pH 7.4) supplemented with 100 μM dtpa, 100 μM Trolox, and 1–100 μM FNOCT **14** at 37°. Fluorescence intensity at λ_{exc} 320 nm, λ_{em} 380 nm was followed over time (sampling interval 60–120 s) using a fluorescence microplate reader. After establishing baseline fluorescence,

MAHMA NONOate (20 nm–100 μM) was added from a freshly prepared stock soln. (in dilute NaOH). Fluorescence given in the figures was assessed after a plateau was reached following complete decomposition of the MAHMA NONOate and was corrected for background fluorescence (same buffer with the same additives and the same FNOCT concentration without added MAHMA NONOate).

Cell Isolation and Cell Culture. Alveolar macrophages were isolated from male *Wistar* rats (350–380 g) by bronchoalveolar lavage as described previously [33]. The cells were seeded on to two 4-well cell culture plates (*Nunc*) and cultured in *Dulbecco's modified Eagles medium* (DMEM) supplemented with L-glutamine (2 mM) and gentamicin (50 $\mu\text{g}/\text{ml}$). One hour after seeding, cells were washed with warm *Hanks'* balanced salt soln. (HBSS; 137 mM NaCl, 5.4 mM KCl, 1.0 mM CaCl₂, 0.5 mM MgCl₂, 0.4 mM KH₂PO₄, 0.3 mM Na₂HPO₄, 25 mM *Hepes* (=4-(2-hydroxyethyl)piperazine-1-ethanesulfonic acid), pH 7.4) and supplied with fresh medium (DMEM) supplemented with L-glutamine (2 mM), gentamicin (50 $\mu\text{g}/\text{ml}$), and 10% heat-inactivated fetal calf serum.

NO Trapping from Alveolar Macrophages. Four to five hours after cell isolation and 18 h prior to the experiments, cells in half of the wells were primed for NO production by the addition of lipopolysaccharides (LPS; 0.5 $\mu\text{g}/\text{ml}$) for 18 h. For experiments, cells were washed with HBSS, counted, and supplied with *Krebs–Henseleit* buffer (115 mM NaCl, 25 mM NaHCO₃, 5.9 mM KCl, 1.2 mM MgCl₂, 1.2 mM NaH₂PO₄, 1.2 mM Na₂SO₄, 2.5 mM CaCl₂, 20 mM *Hepes*, pH 7.4) supplemented with 10 mM D-glucose, 100 μM dtpa, 100 μM *Trolox*, and 10 μM FNOCT **14**; cell density in the experiments was $5.4 \pm 0.5 \cdot 10^4$ cells cm^{-2} ($1.0 \pm 0.1 \cdot 10^5$ cells/well). To half of the wells with activated and half of the wells with nonactivated cells, L-arginine (0.5 mM) was added, to the other wells NMA (0.1 mM) was added. Cells were incubated at 37° in a humidified atmosphere containing 95% air/5% CO₂ for 1 h. After 1 h of incubation, the supernatant was removed and assessed in the microplate reader at λ_{exc} 320 nm, λ_{em} 380 nm by using the same instrument settings as for the cell-free experiments. Cells were lysed in HBSS containing sodium dodecyl sulfate (SDS) in a final concentration of 0.4% (*w/v*), dtpa, and *Trolox*. Cell lysates were centrifuged to remove cell debris, and supernatants were then assessed in the same way as the samples of the supernatant *Krebs–Henseleit* buffer. Blanks of all solns. with all additives including FNOCT **14** were incubated (in the absence of cells) for the same time periods and measured at the same time as samples. Blank values were subtracted from all sample values. Cell blanks were incubated in the absence of FNOCT; however, cellular autofluorescence proved to be negligible in the experimental setting used here. Fluorescence values obtained are either given as arbitrary units (corrected for the fluorescence of blanks, for volume, and cell density) or were corrected for blanks, converted to NO concentrations based on the calibration curve shown in *Fig. 7*, and then corrected for volumes and cell density. After fluorescence of cellular supernatants and cellular lysates was determined, MAHMA NONOate was added in large excess (100 μM) to all samples to obtain maximal FNOCT **14** fluorescence; these values were used to determine FNOCT **14** distribution (supernatant vs. cell-associated).

REFERENCES

- [1] 'The Biology of Nitric Oxide', Eds. S. Moncada, M. Feelisch, R. Busse, and E. A. Higgs, Vol. 3 and 4, Portland Press, London, 1994.
- [2] M. Marzinzig, A. K. Nüssler, J. Stadler, E. Marzinzig, W. Barthlen, N. C. Nüssler, H. G. Beger, S. M. Morris, Jr., U. B. Brückner, *Nitric Oxide: Biol. Chem.* **1997**, *1*, 177.
- [3] R. F. Furchgott, *Angew. Chem., Int. Ed.* **1999**, *38*, 1870.
- [4] F. Murad, *Angew. Chem., Int. Ed.* **1999**, *38*, 1856.
- [5] L. J. Ignarro, *Angew. Chem., Int. Ed.* **1999**, *38*, 1882.
- [6] 'Nitric Oxide, Part A: Sources and Detection of NO; NO Synthase', Ed. L. Packer, in 'Methods in Enzymology', Vol. 268, Academic Press, 1996.
- [7] H.-G. Korth, K. U. Ingold, R. Sustmann, H. de Groot, H. Sies, *Angew. Chem., Int. Ed. Engl.* **1992**, *31*, 891.
- [8] H.-G. Korth, K. U. Ingold, R. Sustmann, H. de Groot, H. Sies, *Angew. Chem.* **1992**, *104*, 915.
- [9] H.-G. Korth, R. Sustmann, P. Lommès, T. Paul, A. Ernst, H. de Groot, L. Hughes, K. U. Ingold, *J. Am. Chem. Soc.* **1994**, *116*, 2767.

- [10] H.-G. Korth, R. Sustmann, P. Lommes, T. Paul, A. Ernst, K. U. Ingold, L. Hughes, H. de Groot, H. Sies, in 'The Biology of Nitric Oxide', Vol. 4, Eds. S. Moncada, M. Feelisch, R. Busse, and E. A. Higgs, Portland Press, London, 1994, p. 220–224.
- [11] D. W. Jones, A. Pomfret, *J. Chem. Soc. Perkin, Trans. 1* **1991**, 263.
- [12] M. Bätz, Ph. D. Thesis, Universität Essen, 1997.
- [13] I. Ioannidis, M. Bätz, T. Paul, H.-G. Korth, R. Sustmann, H. de Groot, *Biochem. J.* **1996**, *318*, 789.
- [14] S. A. Green, D. J. Simpson, G. Zhou, P. S. Ho, N. V. Blough, *J. Am. Chem. Soc.* **1990**, *112*, 7337.
- [15] P. Meineke, U. Rauen, H. de Groot, H.-G. Korth, R. Sustmann, *Chem.–Eur. J.* **1999**, *5*, 1738.
- [16] A. B. A. Jansen, T. J. Russell, *J. Chem. Soc.* **1965**, 2127.
- [17] H. Ferres, *Chem. Ind.* **1980**, 435.
- [18] R. Y. Tsien, *Nature (London)* **1981**, *290*, 527.
- [19] P. Talbiersky, Diploma Thesis, Universität Duisburg-Essen, 2006.
- [20] J. L. Segura, N. Martin, *Chem. Rev.* **1999**, *99*, 3199.
- [21] M. Bätz, H.-G. Korth, R. Sustmann, *Angew. Chem., Int. Ed.* **1997**, *36*, 1501.
- [22] A. R. Forrester, in 'Landolt-Börnstein New Series, Magnetic Properties of Free Radicals', Vol. II/9, Part c1, Eds. H. Fischer and K. H. Hellwege, Springer Verlag, Berlin, 1979.
- [23] P. Meineke, U. Rauen, H. de Groot, H.-G. Korth, R. Sustmann, *Biol. Chem.* **2000**, *381*, 575.
- [24] J. A. Hrabie, J. R. Klose, D. A. Wink, L. K. Keefer, *J. Org. Chem.* **1993**, *58*, 1472.
- [25] A. Werner, *Ber. Dtsch. Chem. Ges.* **1904**, *37*, 3083.
- [26] K. Brass, E. Ferber, *Chem. Ber.* **1922**, *55*, 541.
- [27] J. Schmidt, O. Spoun, *Chem. Ber.* **1922**, *55*, 1194.
- [28] W. Dilthey, I. ter Horst, W. Schommer, *J. Prakt. Chem. N. F.* **1935**, *143*, 189.
- [29] M. Neuenschwander, R. Iseli, *Helv. Chim Acta* **1977**, *60*, 1061.
- [30] H. Koch, *Monatsh. Chem.* **1962**, *93*, 1343.
- [31] H. Koch, L. Katlan, K. Markut, *Monatsh. Chem.* **1965**, *96*, 1646.
- [32] D. R. Duling, *J. Magn. Reson. B* **1994**, *104*, 105.
- [33] J.-F. Wang, P. Komarov, H. de Groot, *Arch. Biochem. Biophys.* **1993**, *304*, 189.

Received April 25, 2006